



**HAL**  
open science

## Imaging of spinor gases

Iacopo Carusotto, Erich Mueller

► **To cite this version:**

Iacopo Carusotto, Erich Mueller. Imaging of spinor gases. *Journal of Physics B: Atomic, Molecular and Optical Physics*, 2004, 37, pp.S115 - S125. 10.1088/0953-4075/37/7/058 . hal-00000797v2

**HAL Id: hal-00000797**

**<https://hal.science/hal-00000797v2>**

Submitted on 13 Jan 2004

**HAL** is a multi-disciplinary open access archive for the deposit and dissemination of scientific research documents, whether they are published or not. The documents may come from teaching and research institutions in France or abroad, or from public or private research centers.

L'archive ouverte pluridisciplinaire **HAL**, est destinée au dépôt et à la diffusion de documents scientifiques de niveau recherche, publiés ou non, émanant des établissements d'enseignement et de recherche français ou étrangers, des laboratoires publics ou privés.

# Imaging of spinor gases

Iacopo Carusotto<sup>1,2</sup> and Erich J. Mueller<sup>3</sup>

<sup>1</sup>*Laboratoire Kastler Brossel, École Normale Supérieure,  
24 rue Lhomond, 75231 Paris Cedex 05, France*

<sup>2</sup>*BEC-INFM Research and Development Center, I-38050 Povo, Trento, Italy*

<sup>3</sup>*Laboratory of Atomic and Solid State Physics, Cornell University, Ithaca, New York 14853*

(Dated: January 13, 2004)

We explore the dielectric properties of spinor condensates. Gases with vector (nematic) order, such as spin-1 condensates with ferromagnetic (antiferromagnetic) interactions, display optical activity (birefringence). This optical activity/birefringence is respectively seen for light detuned from resonance by a frequency which is not too large compared with the fine/hyperfine structure. Careful tuning of the light frequency can isolate either of these two effects. These features can be used to image spin textures in clouds of spin 1 bosons, and to discern states showing different types of spin order.

PACS numbers: 03.75.Mn, 42.30.-d, 03.75.Lm

## I. INTRODUCTION

Superfluids display dramatic rotational properties. For example, arrays of quantized vortices have been observed in rotating gaseous spin-polarized <sup>87</sup>Rb and <sup>23</sup>Na Bose-Einstein condensates (BECs) [1]. The physics of rotating systems is even richer in the presence of spin degrees of freedom: thanks to the interplay of the spin and translational degrees of freedom, simple vortices are replaced by more complicated spin textures. These textures have been studied in many different contexts, from <sup>3</sup>He-A [2] to quantum Hall systems [3] and, more recently, trapped gaseous BECs [4, 5, 6, 7]. They are closely related to three dimensional skyrmion and hedgehog structures which could be engineered in clouds of trapped atoms [8].

Theoretical studies have analyzed the structure of spin textures in rotating spinor BECs for different values of the spin, the trap rotation frequency, and the atom-atom interactions [4, 5]. Experimental studies, beginning with pseudo-spin-1/2 systems [6] and continuing with spin-1 and spin-2 condensates [7], have observed individual spin textures. These experiments are complemented by studies of spin dynamics in non-rotating spin-1 and spin-2 clouds [9].

In most of these experiments [10], imaging is performed by first separating the different spin components using a magnetic field gradient (the method pioneered by Stern and Gerlach [11]). The spin components are then separately imaged via conventional optical absorption or phase contrast techniques. This approach is intrinsically destructive and is unable to probe coherences between the different spin components. Moreover, images of the individual components are very sensitive to global rotations of the order parameter [5].

In the present paper, we propose a different imaging scheme which is predicted to provide non-destructive, *in-situ*, images of the spin textures and which directly addresses the geometrical features of the BEC order parameter (density, spin, and nematicity profiles) rather than its components in some specific basis. The method re-

lies on the dependence of the dielectric properties of a spinor atomic gas on the internal state of the atoms. Focussing our attention on the case of spin-1 atoms, we derive a simple expression for the local dielectric tensor  $\epsilon_{ij}(\mathbf{x})$  in terms of the local density  $\rho(\mathbf{x})$ , spin density  $\mathbf{S}(\mathbf{x})$ , and quadrupolar (nematic) order parameter  $N_{ij}(\mathbf{x})$  of the atomic gas. Using this expression for  $\epsilon_{ij}(\mathbf{x})$ , we then study the propagation of polarized light across an atomic cloud: we show how information about the spatial profile of the spin texture can be retrieved by analyzing the intensity, phase, and polarization profile of the transmitted light. Our technique has analogies in other areas of condensed matter physics: the polarization of the electrons in a solid-state sample [12] as well as the order parameter of nematic liquid crystals [13] can be measured by looking at polarization changes in a transmitted, diffracted, or reflected light. As the order parameter of spin-1 atomic systems is a three-component complex field, it can simultaneously have non-vanishing vector (spin) and tensor (nematic) components: we discuss possible ways of isolating the contribution of each of them.

## II. THE LIGHT-MATTER COUPLING HAMILTONIAN

The electric-dipole Hamiltonian describing the interaction of light with a two-level atom can be written in a second-quantized form as:

$$H_{\text{int}} = - \int d\mathbf{x} \sum_{\eta i \alpha} D_{\eta i \alpha} \hat{\phi}_{\eta}^{\dagger}(\mathbf{x}) \hat{E}_i(\mathbf{x}) \hat{\psi}_{\alpha}(\mathbf{x}). \quad (1)$$

The atomic field operators  $\hat{\phi}_{\eta}(\mathbf{x})$  and  $\hat{\psi}_{\alpha}(\mathbf{x})$  destroy an atom at spatial position  $\mathbf{x}$  in respectively the  $\eta$  sublevel of the excited state or the  $\alpha$  sublevel of the ground state.  $\hat{E}_i(\mathbf{x})$  is the  $i$ -component of the electric field operator at  $\mathbf{x}$  and  $D_{\eta i \alpha} = \langle e : \eta | d_i | g : \alpha \rangle$  gives the matrix element of the  $i$ -component of the electric dipole moment

ccsd-00000797 (version 2) : 13 Jan 2004

between the sublevels  $\eta$  and  $\alpha$  of respectively the excited and ground state.

For light frequencies  $\omega$  well detuned from the resonance frequency  $\omega_0$  of the  $g \rightarrow e$  transition, we can eliminate the excited state and write an effective Hamiltonian for the ground state atoms coupled to the electromagnetic field:

$$H_{\text{int}} = \int d\mathbf{x} \sum_{\alpha i j \beta} U_{\alpha i j \beta} \hat{\psi}_\alpha^\dagger(\mathbf{x}) \hat{E}_i^\dagger(\mathbf{x}) \hat{E}_j(\mathbf{x}) \hat{\psi}_\beta(\mathbf{x}), \quad (2)$$

where the  $U$  tensor is defined as:

$$U_{\alpha i j \beta} = \frac{1}{\hbar(\omega - \omega_0)} \sum_{\eta} D_{\eta i \alpha}^* D_{\eta j \beta}, \quad (3)$$

the indices  $\alpha$  and  $\beta$  run over the ground state sublevels and  $\eta$  runs over the excited state sublevels.

In our case of spin 1 atoms, the matter field is a three-component vector and can be written in terms of its (operator-valued) Cartesian components as  $\vec{\psi} = (\hat{\psi}_x, \hat{\psi}_y, \hat{\psi}_z)$  [14]. The local one-body density-matrix  $m_{ij}(\mathbf{x}) = \hat{\psi}_i^\dagger(\mathbf{x}) \hat{\psi}_j(\mathbf{x})$  is the tensor product of the two distinct spin 1 objects  $\vec{\psi}$  and  $\vec{\psi}^\dagger$ , so it can be represented in terms of three irreducible tensor components with angular momentum 0, 1 and 2. Their explicit expressions in Cartesian components are:

$$\rho(\mathbf{x}) = \sum_j m_{jj}(\mathbf{x}) = \vec{\psi}^\dagger(\mathbf{x}) \cdot \vec{\psi}(\mathbf{x}) \quad (4)$$

$$S_j(\mathbf{x}) = -i \varepsilon_{jkl} m_{kl}(\mathbf{x}) = -i \vec{\psi}^\dagger(\mathbf{x}) \times \vec{\psi}(\mathbf{x}) \Big|_j \quad (5)$$

$$N_{ij}(\mathbf{x}) = \frac{1}{2} [m_{ij}(\mathbf{x}) + m_{ji}(\mathbf{x})] - \frac{\rho(\mathbf{x})}{3} \delta_{ij}. \quad (6)$$

The totally antisymmetric unit tensor is denoted  $\varepsilon_{jkl}$ . Physically, the scalar  $\rho$  corresponds to the total density, the vector  $\mathbf{S}$  to the spin density, and the second-rank, symmetric tensor  $N$  to the *nematicity* (or quadrupole moment). An identical decomposition into the intensity  $I$ , the spin density  $\Sigma$  and the nematicity  $\mathcal{N}$  can be performed for the electromagnetic field one-body density matrix defined as  $f_{ij} = \hat{E}_i^\dagger \hat{E}_j$ .

As we assume no external field is present to break rotational invariance, the Hamiltonian is a scalar (that is spin 0) object. Scalar objects can be found in the tensor product of two quantities only if the two quantities have the same spin. This implies that the Hamiltonian (2) can be decomposed in the form:

$$H_{\text{int}} = \int d\mathbf{x} \left[ b_0 I(\mathbf{x}) \rho(\mathbf{x}) + b_1 \Sigma(\mathbf{x}) \cdot \mathbf{S}(\mathbf{x}) + b_2 \sum_{ij} \mathcal{N}_{ij}(\mathbf{x}) N_{ij}(\mathbf{x}) \right], \quad (7)$$

where the three real coefficients  $b_{0,1,2}$  depend on the internal structure of the atom and on the frequency of the

light. Comparing (7) with (2), one finds

$$b_0 = \frac{1}{9} \sum_{\alpha\beta} U_{\alpha\beta\beta\alpha} \quad (8)$$

$$b_1 = \frac{1}{12} \sum_{\alpha\beta} (U_{\alpha\beta\alpha\beta} - U_{\alpha\alpha\beta\beta}) \quad (9)$$

$$b_2 = \frac{1}{6} \sum_{\alpha\beta} (U_{\alpha\beta\alpha\beta} + U_{\alpha\alpha\beta\beta}) - \frac{1}{3} \sum_{\alpha} U_{\alpha\alpha\alpha\alpha}. \quad (10)$$

In the next section, we give explicit expressions for the  $U$  tensor and the  $b_i$  coefficients for a few simple cases.

### III. THE DIELECTRIC TENSOR OF A SPIN 1 GAS

The form (7) of the light-matter Hamiltonian can be used for studying the optical potential induced by light on atoms, as well as the refractive index observed by light while crossing the atomic sample.

In the first case, a scalar potential comes from the local intensity  $I(\mathbf{x})$  of light, a pseudo-magnetic field comes from the electromagnetic spin  $\Sigma(\mathbf{x})$ , and the  $\mathcal{N}(\mathbf{x})$  tensor couples to the nematicity  $N(\mathbf{x})$  of the atoms. A first application of this formalism has been given in [17], where effects arising from a kind of spin-orbit coupling induced by the pseudo-magnetic field are analyzed for atoms propagating in suitably designed optical lattices.

In the present paper, we concentrate on the second class of phenomena, namely on how the optical properties of the atomic cloud depend on the spin state of the atoms; in particular we shall discuss how the polarization state of a light beam after crossing the atomic sample can be used to obtain information on the spin state of the atoms.

#### A. The general structure of the dielectric tensor

Under a mean-field approximation in which the quantum correlations between the matter and the light field are neglected, a wave equation for the eigenmodes of the electromagnetic field in a homogeneous medium can be directly obtained from the Hamiltonian (2):

$$(\hbar\omega(\mathbf{1} - \lambda) - \hbar ck P_\perp) \mathbf{E} = 0 \quad (11)$$

where  $\mathbf{1}$  is the identity matrix, the projector  $P_\perp$  projects orthogonally to the wavevector  $\mathbf{k}$  and the tensor  $\lambda$  has been defined as:

$$\lambda_{jk} = \frac{1}{\epsilon_0} U_{ijkl} \langle m_{il} \rangle, \quad (12)$$

where  $\epsilon_0$  ( $= 1/4\pi$  in cgs units) is the permittivity of free space. By comparing this wave equation with the Fresnel equation for a generic medium of dielectric tensor  $\epsilon$ :

$$\left( \frac{\omega^2}{c^2} \epsilon - k^2 P_\perp \right) \mathbf{E} = 0, \quad (13)$$

one obtains the following explicit expression for the dielectric tensor of the atomic sample at the frequency  $\omega$  in terms of the coupling tensor  $U$  in the Cartesian basis and the one-body density matrix  $m$ :

$$\epsilon_{jk} = \delta_{jk} - \frac{2}{\epsilon_0} U_{ijkl} \langle m_{il} \rangle. \quad (14)$$

The same symmetry arguments previously used to parametrize the Hamiltonian in the form (7) lead to the following expression of the dielectric tensor (14):

$$\epsilon_{jk} = \delta_{jk} + c_0 \langle \rho \rangle \delta_{jk} - i c_1 \epsilon_{jkl} \langle S_l \rangle + c_2 \langle N_{jk} \rangle, \quad (15)$$

where  $c_j = -2b_j/\epsilon_0$ . The scalar term proportional to  $c_0$  corresponds to the isotropic polarizability of the atoms, while the vector term proportional to  $c_1$  describes their optical activity around the axis defined by the atomic spin  $\mathbf{S}$ . Finally, the tensor term proportional to  $c_2$  gives birefringence effects, whose principal axis coincide with the ones of the nematicity ellipsoid defined as:

$$(N_{ij} + \frac{\rho}{3} \delta_{ij}) x_i x_j = 1. \quad (16)$$

The matrix elements  $D_{ijk}$ , and hence the coefficients  $c_j$  can be related to the line width  $\Gamma$  of the atomic transition [18]. For the fundamental  $D_{1,2}$  transitions of a typical alkali atom such as  $^{23}\text{Na}$  or  $^{87}\text{Rb}$ ,  $\Gamma \approx 5 \cdot 10^7 \text{s}^{-1}$  and  $|c_j| \approx 10^{-15} \text{cm}^3 \Gamma / |\omega - \omega_0|$ . A typical *in-situ* imaging setup [19] uses detunings in the GHz range (which are large enough that absorption effects can be ignored [20]), and atomic densities of order  $10^{14} \text{cm}^{-3}$ , resulting in a dielectric tensor which differs from unity by an amount of magnitude  $|\epsilon - 1| \approx 10^{-2}$ . As we shall see in section III C, quantum interference effects can drastically reduce the magnitude of any given  $c_j$  in some specific frequency domains.

## B. The dielectric tensor for a single transition

The coefficients  $c_i$  in the parametrization (15) of the dielectric tensor depend on the internal structure of the atom. Since the ground state has been assumed to have spin  $F_g = 1$ , absorbing a photon can bring the atoms into excited states of angular momentum  $F_e = 0, 1, 2$ . In the present subsection, we shall derive a simple expression of the  $c_i$  coefficients in terms of the strength of the optical transition for the case where only one excited multiplet is involved. For notational simplicity we omit the angular brackets denoting expectation values of matter field operators.

For  $F_e = 0$ , the  $D$  tensor in Cartesian components ( $j, k = \{x, y, z\}$ ) has the form  $D_{0jk} = D_0 \delta_{jk}$ , so the dielectric tensor is:

$$\epsilon_{jk} = \delta_{jk} + A_0 m_{jk} = \delta_{jk} + A_0 \left[ \frac{\rho}{3} \delta_{jk} + \frac{i}{2} \epsilon_{jkl} S_l + N_{jk} \right], \quad (17)$$

i.e.  $c_0^{(0)} = A_0/3$ ,  $c_1^{(0)} = -A_0/2$ , and  $c_2^{(0)} = A_0$  with  $A_0 = -2|D_0|^2/\epsilon_0 \hbar(\omega - \omega_0)$ . This result has a simple interpretation: a photon polarized along the Cartesian axis  $j$  interacts only with the component of the matter field along the same axis.

For  $F_e = 1$ , the Cartesian ( $j, k, l = \{x, y, z\}$ ) components of the  $D$  tensor have the form  $D_{jkl} = D_1 \epsilon_{jkl}$  and therefore one has:

$$\begin{aligned} \epsilon_{jk} &= \delta_{jk} + A_1 [\rho \delta_{jk} - m_{kj}] \\ &= \delta_{jk} + A_1 \left[ \frac{2}{3} \rho \delta_{jk} + \frac{i}{2} \epsilon_{jkl} S_l - N_{jk} \right], \end{aligned} \quad (18)$$

i.e.  $c_0^{(1)} = 2A_1/3$ ,  $c_1^{(1)} = -A_1/2$ , and  $c_2^{(1)} = -A_1$  with  $A_1 = -2|D_1|^2/\epsilon_0 \hbar(\omega - \omega_0)$ . In physical terms, this means that light interacts only with the matter field polarized along direction orthogonal to the electric field polarization.

Finally, for  $F_e = 2$ , the dielectric tensor has the form:

$$\begin{aligned} \epsilon_{jk} &= A_2 \left[ \frac{1}{2} \rho \delta_{jk} + \frac{1}{2} m_{kj} - \frac{1}{3} m_{jk} \right] \\ &= A_2 \left[ \frac{5}{9} \rho \delta_{jk} - \frac{5i}{12} \epsilon_{jkl} S_l + \frac{1}{6} N_{jk} \right], \end{aligned} \quad (19)$$

i.e.  $c_0^{(2)} = 5A_2/9$ ,  $c_1^{(2)} = 5A_2/12$ , and  $c_2^{(2)} = A_2/6$ . The coefficient  $A_2$  can be obtained from the electric dipole moment  $D_2$  of the optical transition of the  $F_g = 1 \rightarrow F_e = 2$  transition as  $A_2 = -2|D_2|^2/\epsilon_0 \hbar(\omega - \omega_0)$ . More specifically,  $D_2$  is defined as the electric dipole matrix element between the  $m_F = 1$  sublevel of the ground state and the  $m_F = 2$  sublevel of the excited state. The matrix elements of the transitions between the other sublevels are related to  $D_2$  by the appropriate Clebsch-Gordan coefficients.

## C. Effect of the fine and hyperfine structures of the atom

If more than one excited state is involved in the optical process, the effective coupling  $U$  of the ground state atoms to the light is given by the sum of the contributions (3) of each single excited state, each of them being weighted by a factor  $1/(\omega_i - \omega)$ , where  $\hbar\omega_i$  is the excitation energy and  $\omega$  the light frequency. Clearly, the result will be dominated by the states which are closest to resonance. By tuning to frequencies where the contributions from different excited states cancel, one can take advantage of quantum interference effects to make at least one of the coefficients  $c_{0,1,2}$  vanish.

For example, considerable simplification is found if the detuning is large compared to either the fine or hyperfine splitting. Consider the fundamental  $nS \rightarrow nP$  transition of an alkali atom such as  $^{23}\text{Na}$  or  $^{87}\text{Rb}$ : the  $S = 1/2$  electronic spin couples to the excited state's  $L = 1$  electronic orbital angular momentum to produce two fine components of total electronic angular momentum  $J = 1/2$  or

3/2. The ground state, having instead a vanishing orbital angular momentum  $L = 0$ , contains a single fine component of total electronic angular momentum  $J = 1/2$ . Both  $^{23}\text{Na}$  and  $^{87}\text{Rb}$  have a nuclear spin of  $I = 3/2$ : coupling between the nuclear and electronic spins therefore result in the ground state splitting into two hyperfine components with  $F = 2$  and  $F = 1$  (in this paper we limit ourselves to  $F = 1$ ). The  $J = 1/2, 3/2$  fine components of the excited state respectively split into two hyperfine components of  $F = 1, 2$ , and four hyperfine components of  $F = 0, 1, 2, 3$ . For these alkali atoms, the fine structure separation between the  $D_1$  ( $S_{1/2} \rightarrow P_{1/2}$ ) and  $D_2$  ( $S_{1/2} \rightarrow P_{3/2}$ ) lines is of the order of THz. Hyperfine structure, resulting from the much weaker coupling between the electron and the nucleus, amounts to a few GHz for the electronic ground state and to a fraction of GHz for the excited state [21].

If the detuning  $\Delta$  of the light is much larger than the hyperfine splitting  $\Delta_{\text{HF}}$ , the nucleus, whose direct coupling to radiation is extremely weak, is not expected to play any role in the dynamics. In this regime, the frequency denominators in the contributions (3) to the  $U$  tensor coming from the different hyperfine components are approximately equal. Consequently,  $U$  acts as the identity matrix in the space of nuclear states. It immediately follows that the dielectric tensor (14) only depends on the electronic part of the atomic density matrix,  $m^{(e)} = \text{Tr}_n[m] = \sum_{m_I} \langle m_I | m | m_I \rangle$ , where the index  $m_I$  runs over the  $2I + 1$  possible nuclear spin states. As the total electronic angular momentum of the ground state is  $J = 1/2$ , the decomposition analogous to the ones in (7) and (15) now gives two components of angular momentum respectively 0 and 1, but no component of angular momentum 2. In physical terms, this means that, once the sum over the hyperfine components of the excited state is performed, one has  $c_2 = b_2 = 0$  and no birefringence effect nor any mechanical coupling of light to the nematic order parameter  $N$  can be present. The coefficients  $c_1$  and  $c_0$  will, however, generally be non-zero [22]. For a large but finite detuning as compared with the hyperfine splitting, the ratio  $c_2/c_{1,0}$  scales as  $\Delta_{\text{HF}}/\Delta$ .

If the detuning of the light is also large with respect to the fine-structure splitting, then one can neglect the coupling between light and the electronic spin. The sum in (3) then traces out all of the spin degrees of freedom (both electronic and nuclear), leaving only the electronic orbital angular momentum. Consequently, in addition to  $c_2 = b_2 = 0$ , we have  $c_1 = b_1 = 0$ , and the atoms behave as a gas of spherically symmetric scatterers, with an isotropic dielectric tensor. In this regime, the mechanical coupling between light and the atoms does not depend on their initial state. This effect is currently exploited in optical traps in order to obtain a confining potential which traps all spin states in the same way [15].

#### IV. THE IMAGING METHOD

The simple dependence of the dielectric tensor on the spin and nematic order parameters (15) is an useful starting point for optically imaging the order parameter of a spin 1 atomic sample. As a simple example, consider a thin, pancake-shaped, Bose-Einstein condensate which is rotating around the symmetry axis  $\hat{z}$ . Depending on the relative value of the s-wave scattering lengths  $a_{0,2}$  in respectively the singlet and quintuplet channels, the ground state of the system in the rotating frame show completely different textures [5]. As two specific examples, figs.1a and 2a show the nematicity and spin and patterns for the antiferromagnetic case,  $a_0 < a_2$ , and the ferromagnetic case,  $a_2 < a_0$ . In the former case, the condensate shows defects such as  $\pi$ -dislocations in the nematic order parameter  $N$ , while the spin  $\mathbf{S}$  vanishes outside of the cores of these defects. In the latter case, the condensate shows a spin pattern, while the nematicity ellipsoids are pancake shaped, with their minor axis aligned with the local spin.

We imagine that the imaging beam propagates along  $\hat{z}$ , i.e. parallel to the rotation axis, and its polarization before interacting with the atoms is given by the two-component, generally complex, polarization vector  $\mathbf{p}_{in} = (p_x, p_y)$ . We assume the cloud is optically thin and that the length scale of the spin pattern is much larger than the optical wavelength used for the imaging, so that diffraction effects during the propagation through the cloud can be neglected and the atomic density matrix  $m$  can be treated as locally uniform. These assumptions are valid for sufficiently detuned light (for typical atomic densities it suffices that  $|\omega - \omega_0| > 100$  MHz) and sufficiently weak traps ( $\omega_{\text{ho}} \sim 10$  Hz). Smaller scale feature can be imaged by allowing the cloud to expand ballistically before imaging.

The polarization of the transmitted beam at the transverse position  $\mathbf{x}_\perp$  after propagation through the cloud is given by the following expression in terms of a column integral along the line of sight:

$$\mathbf{p}_{out}(\mathbf{x}_\perp) = e^{i\omega z/c} \left[ \mathbf{1} + \frac{i\omega}{c} \int dz (n(\mathbf{x}_\perp, z) - \mathbf{1}) \right] \mathbf{p}_{in}. \quad (20)$$

The assumption that the cloud is optically thin implies that the magnitude of the term involving the integral is much smaller than unity. The matrix giving the local refractive index at the spatial position  $(\mathbf{x}_\perp, z)$ , is defined as the square root  $n(\mathbf{x}_\perp, z) = \sqrt{\epsilon^{(xy)}}$  of the reduced dielectric tensor  $\epsilon^{(xy)}$  in the  $(xy)$  plane, defined as  $\epsilon^{(xy)} = P_\perp \epsilon P_\perp$  where  $P_\perp$  is the projection operator orthogonal to the  $\hat{z}$  axis. As one can easily see from (15),  $\epsilon^{(xy)}$  depends on the density  $\rho$ , on the  $S_z$  component of the spin and on the  $N_{xx,yy,xy,yx}$  components of the nematic order parameter only.

If the incident beam is circularly polarized  $\sigma_\pm$ , the density  $\rho$  and the spin component  $S_z$  both only give a phase shift. On the other hand, the nematicity can mix the two

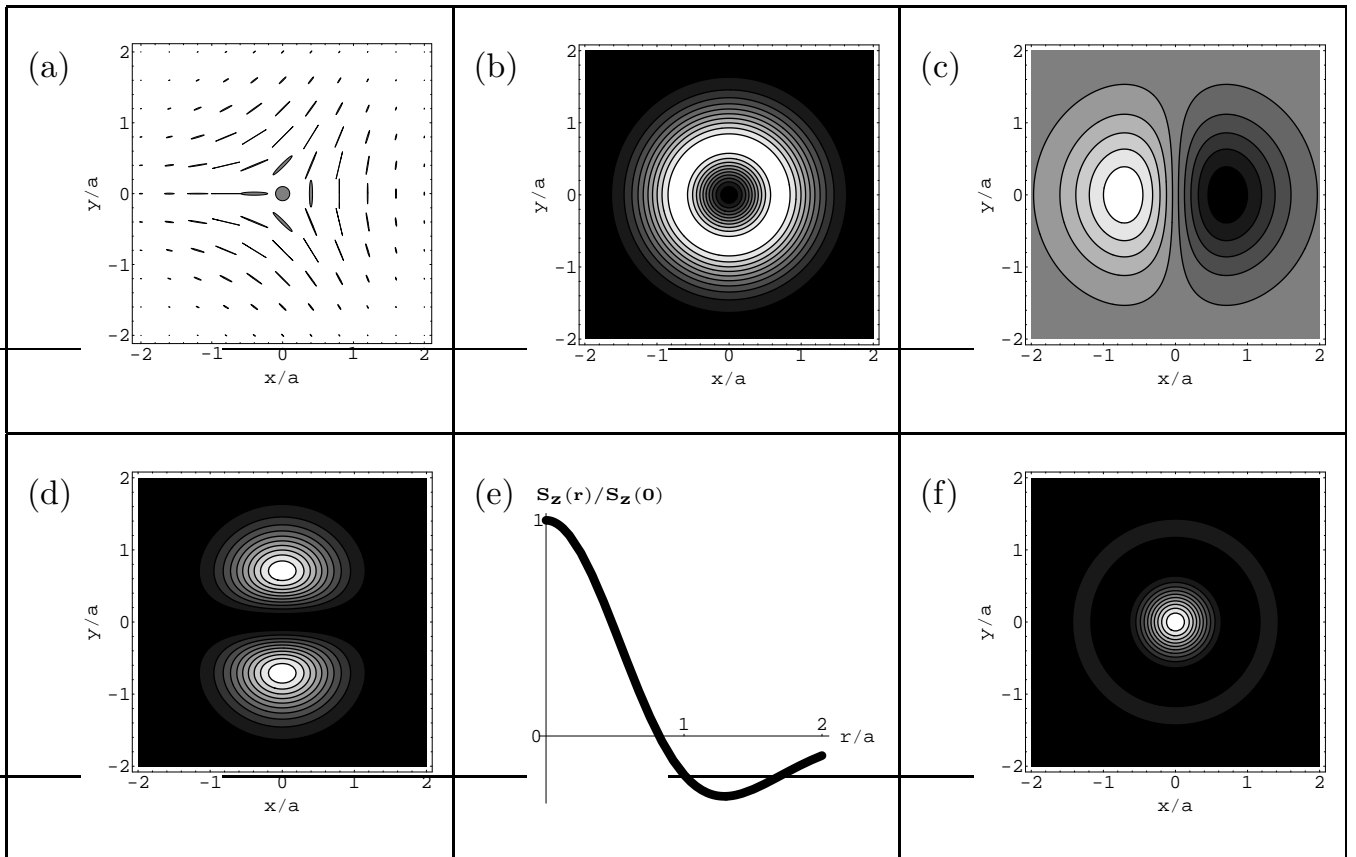


FIG. 1: Nematic order of a  $\pi$  disclination in a rotating spinor BEC with weak antiferromagnetic interactions after free expansion for time  $t$ . The lengthscale is given by  $a = d_{\text{ho}}\sqrt{1 + (\omega_{\text{ho}}t)^2}$ , where  $d_{\text{ho}} = \sqrt{\hbar/m\omega_{\text{ho}}}$ , and  $\omega_{\text{ho}}$  is the frequency of the harmonic trap in which the disclination formed [23]. Typically,  $a \approx 100 \mu\text{m}$ . If  $\omega_{\text{ho}}$  is small enough, then *in-situ* imaging (where  $t = 0$ ) is possible ( $^{87}\text{Rb}$  in an  $\omega_{\text{ho}} = 10\text{s}^{-1}$  trap has  $d_{\text{ho}} = 9 \mu\text{m}$ , and is amenable to *in-situ* imaging). Panel (a): Two dimensional projections of the nematicity ellipsoids (16) are shown on a regular grid. Away from the center the ellipsoids are degenerate and appear as rods. Panel (b,c): Images of the disclination using circularly polarized  $\sigma_+$  probe light. The intensity of the generated  $\sigma_-$  component is shown in (b) and a phase-contrast image after mixing with the incident light (with phase  $\phi = \pi/2$ ) is shown in (c). Panel (d): Image of the disclination using light linearly polarized along  $x$  and a crossed polarizer, when  $c_1 = 0$ . Panel (e): The  $\hat{z}$  component of the spin  $S_z$ , as a function of radial position. Panel (f): Image of the disclination using linearly polarized light and a crossed polarizer when the detuning is much greater than the hyperfine splitting so that  $c_2 = 0$ .

circular polarizations. We assume that the frequency of the imaging light is chosen so to have a significant coupling  $c_2$  to the nematicity  $N$  (see Appendix). If one illuminates the cloud with pure  $\sigma_+$  polarized light of amplitude  $\alpha_+^{(0)}$ , the  $\sigma_-$  component of the field after crossing the cloud has the amplitude:

$$\alpha_- = \alpha_+^{(0)} \frac{i\omega c_2}{4c} \int dz [N_{xx} - N_{yy} + i(N_{xy} + N_{yx})]. \quad (21)$$

In geometrical terms, a  $\sigma_-$  component is generated as soon as the (elliptical) cross-section of the nematicity ellipsoid (16) along the  $z = 0$  plane is not circular. After blocking the original  $\sigma_+$  component with a polarizer, the intensity of the transmitted light  $I_- = |\alpha_-|^2$  will be proportional to the square of the column integral of the reduced nematicity parameter

$$\|N\|^2 = (N_{xx} - N_{yy})^2 + \text{Re}[2N_{xy}]^2 \quad (22)$$

along the  $xy$  plane. In fig.1b we have plotted the simulated intensity profile for a  $\pi$  dislocation in a trapped rotating antiferromagnetic ( $a_2 > a_0$ ) spinor condensate. In the  $m_z = (1, 0, -1)$  basis, we have taken a condensate wavefunction of the form:

$$\psi(x, y) = \begin{pmatrix} 1 \\ 0 \\ u(x + iy) \end{pmatrix} \exp\left[-\frac{|x^2 + y^2|}{2d_{\text{ho}}^2}\right] \quad (23)$$

with  $u = 1.22$  and the harmonic oscillator length  $d_{\text{ho}} = \sqrt{\hbar/m\omega_{\text{ho}}}$  is of the order of  $\mu\text{m}$  [5]. The corresponding structure of the nematic order parameter is shown in fig.1a. In this specific case, the magnitude of the nematicity  $\|N\|$  is symmetric under rotations around the  $\hat{z}$  axis. The principal axes of  $N_{ij}$  rotate by  $\pi$  upon circling the disclination center.

More information on the structure of the nematic or-

der parameter can be extracted by using phase-contrast techniques. Denoting with  $0 \leq \theta < \pi$  the angle between the  $\hat{x}$  axis and the minor axis of the nematicity ellipsoid, it follows from (21) that the phase of the generated  $\sigma_-$  component makes an angle  $\pi/2 + 2\theta$  with respect to the incident  $\sigma_+$  component. When this  $\sigma_-$  component is mixed with the incident  $\sigma_+$  component (with a mixing phase  $\phi$ ) in a typical phase-contrast scheme [16], the deviation of the detected intensity from its background value will be proportional to the quadrature  $\text{Re}[e^{i\phi}\alpha_-/\alpha_+^{(0)}]$ . As an example of such an images, we have plotted in fig.1c a simulated image for the  $\phi = \pi/2$  case. The phase of the generated  $\sigma_-$  at points  $\mathbf{x}$  and  $-\mathbf{x}$  differ by  $\pi$  as a result of the different orientation of the nematic order parameter. Changing the mixing phase rotates this image by  $\phi$ .

In experiments on liquid crystals [13], one typically images using linearly polarized light. A crossed polarizer on the other side of the sample selects out the orthogonal component of the transmitted light. If the nematic order parameter is not parallel or perpendicular to the incident polarization plane, the polarization plane is rotated, and light will be transmitted through the crossed polarizer. The same approach can be used here, however, the optically active regions where  $S_z \neq 0$  can also rotate the polarization plane, making it more difficult to analyze the images. One can isolate the contribution from the nematic order by working at a frequency at which the coupling of light to the spin vanishes, *i.e.*  $c_1 = 0$ . A simulated image is shown in fig.1d for incident light polarized along  $x$ : the detected intensity is maximum along the  $\hat{y}$  axis where the nematic order parameter makes an angle  $\pm\pi/4$  with  $\hat{x}$ .

We can isolate the contribution from the atomic spin  $\mathbf{S}$  by working at a detuning which is large compared to the hyperfine structure of the excited state. In this case,  $c_2 = 0$  and there is no mixing of the  $\sigma_{\pm}$  components. The difference between the phase shifts of the  $\sigma_{\pm}$  components results in the rotation of the polarization plane of a linearly polarized beam by an angle  $\theta_{\text{rot}}$ , which depends on the column integral of  $S_z$  as,

$$\theta_{\text{rot}} = \frac{\omega c_1}{2c} \int dz S_z. \quad (24)$$

The intensity of linearly polarized light passing through a crossed polarizer will be proportional to  $\sin^2(\theta_{\text{rot}})$ , which in the limit of an optically thin sample is just  $\theta_{\text{rot}}^2$ . One can thus get a direct measurement of the integrated magnitude of the  $\hat{z}$  component of the atomic spins. In fig.1e,  $S_z$  is plotted for the  $\pi$ -disclination, and in fig.1f, a simulated image is shown.

Since  $\theta_{\text{rot}}$  corresponds to the phase shift between the  $\sigma_{\pm}$  components, one can also measure it via phase contrast techniques. In fig.2c we show a simulated phase contrast image of a texture in a ferromagnetic gas. In the weakly interacting limit [5], this coreless vortex has

a wavefunction in the  $m_z = (1, 0, -1)$  basis given by:

$$\psi(x, y) = \begin{pmatrix} v(x + iy)^2 \\ u(x + iy) \\ 1 \end{pmatrix} \exp\left[-\frac{|x^2 + y^2|}{2d_{\text{ho}}^2}\right] \quad (25)$$

with  $u = -1.03$ ,  $v = 0.81$ , and is illustrated in 2a,b. Again,  $d_{\text{ho}} \approx \mu\text{m}$  is the oscillator length. In the external region, the spins points downwards, while they reverse direction as one approaches the center. Consequently, the image in fig.2c shows a low intensity region at the center, and a higher intensity region on a ring of radius  $1.8a$  ( $= 1.8 d_{\text{ho}}$  for *in-situ* imaging).

If the system shows a repeated pattern of vortices or  $\pi$ -dislocations instead of a single one, the imaging may be better performed in the far-field plane. The amplitude of the Bragg-diffracted light in the direction  $(\mathbf{k}_{\perp}, k_z)$  is proportional to the Fourier transform of the emerging field after interaction with the cloud. As an example, we have plotted in fig.3b the Bragg diffraction pattern for the lattice of  $\pi$ -disclinations shown in fig.3a; the incident light is  $\sigma_+$  polarized and  $\sigma_-$  diffracted light is observed. The periodicity of the lattice results in an evenly spaced series of isolated diffraction peaks whose strengths and geometrical arrangement give the detailed geometry of the lattice.

## V. CONCLUSIONS

In summary, we have presented a novel technique for both the *in-situ* and post-expansion imaging of spin textures in gaseous spin-1 atomic Bose-Einstein condensates. The technique is based on the dependence of the dielectric tensor on the local value of the density and of the spin and nematic order parameters. By considering a series of different spin textures, and detection schemes, we demonstrated how a range of physical quantities, such as the  $z$  component of the spin, and the magnitude and the orientation of the nematic order parameter can be imaged.

This polarized imaging technique can also be used to distinguish between states with and without spin order: both nematic and spin singlet states have been in fact predicted for antiferromagnetically interacting spin-1 atoms in an optical lattice [24].

## Acknowledgments

We acknowledge hospitality at the Benasque Center for Science and the Aspen Center for Physics where most of the present work has been done. I.C. acknowledges a Marie Curie grant from the EU under contract number HPMF-CT-2000-00901. Laboratoire Kastler Brossel is a Unité de Recherche de l'École Normale Supérieure et de l'Université Paris 6, associée au CNRS.

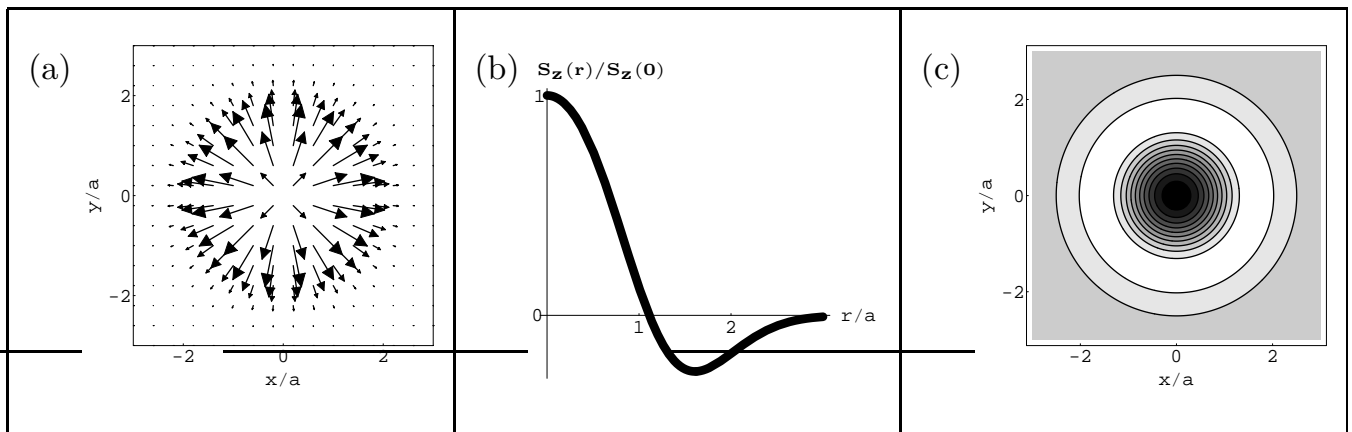


FIG. 2: Panel (a,b): geometrical structure of coreless vortex in a trapped rotating spinor BEC with weak ferromagnetic interactions. Lengthscale  $a$  is explained in figure 1. In (a), arrows represent the in-plane component of the spin, while (b) shows the radial dependance of the  $\hat{z}$  component. Panel (c): image of the coreless vortex by detecting the phase difference between the transmitted  $\sigma_{\pm}$  components.

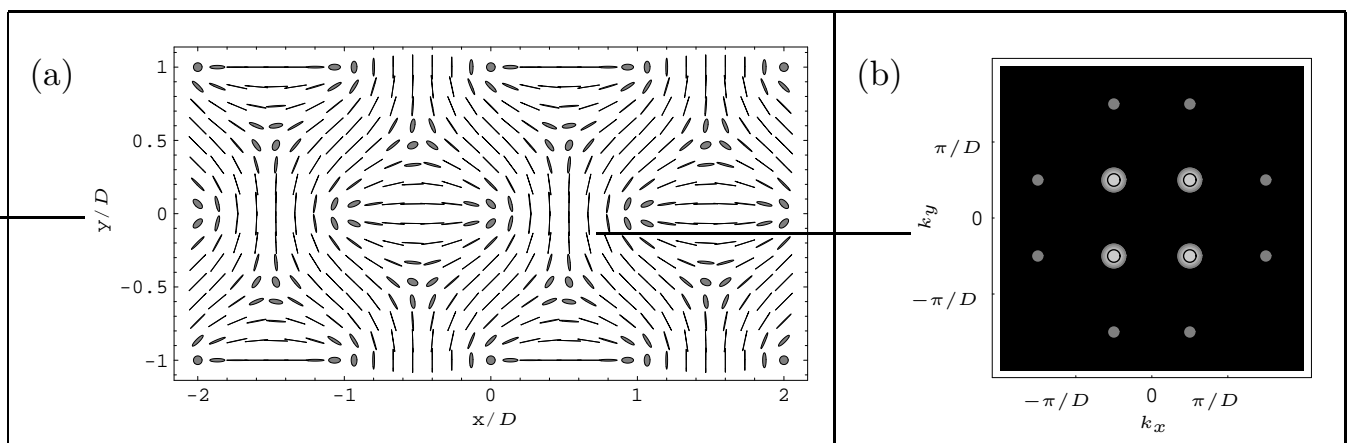


FIG. 3: Panel (a): Nematic order in array of  $\pi$  disclinations. The closest distance between disclinations whose cores have the same spin polarization is  $D = \sqrt{\hbar/m\Omega}$ , where  $\Omega$  is the rotation speed ( $^{23}\text{Na}$  rotating at  $\Omega = 10\text{s}^{-1}$  has  $D = 17\mu\text{m}$ ). As in figure 1, this image scales under free expansion. Panel (b): Diffraction pattern seen in  $\sigma_-$  light when  $\sigma_+$  light is incident on this array of disclinations.  $k_x$  and  $k_y$  are the transverse wave vectors of the diffracted light.

#### APPENDIX A: QUANTITATIVE REMARKS ON ABSORPTION AND THE $c_2$ COUPLING

Dispersive imaging techniques, such as this one, require that absorption is negligible. Minimizing absorption is also crucial if one wishes to make *in-situ* measurements, as the absorption and subsequent spontaneous emission processes heat the sample. The present imaging scheme of the nematic order parameter requires detun-

ings  $\Delta = \omega - \omega_0$  not too large than the hyperfine splitting in order to have a significant coupling  $c_2$  of light to the nematic order parameter.

Since for the  $D_1$  line  $\Delta_{HF}/\Gamma$  is of the order of a few tens [21], absorption can be avoided while still keeping  $c_2/c_{0,1}$  of order unity. These detunings are of the same order as those used in the experiments of [19] and the signals are therefore readily measured.

[1] K. W. Madison, F. Chevy, W. Wohlleben, and J. Dalibard, Phys. Rev. Lett. **84**, 806 (2000); J. R. Abo-Shaer,

C. Raman, J. M. Vogels, and W. Ketterle, Science **292**, 476 (2001); P. C. Haljan, I. Coddington, P. Engels, and

- E. A. Cornell, Phys. Rev. Lett. **87**, 210403 (2001); E. Hodby, G. Hechenblaikner, S. A. Hopkins, O. M. Maragò, and C. J. Foot, Phys. Rev. Lett. **88**, 010405 (2002).
- [2] D. Vollhardt and P. Wölfe, *The Superfluid Phases of He 3* (Taylor & Francis, London, 1990).
- [3] E. H. Aifer, B. B. Goldberg and D. A. Broido, Phys. Rev. Lett. **76**, 680 (1996); S. E. Barrett, G. Dabbagh, L. N. Pfeiffer, K. W. West and R. Tycko, Phys. Rev. Lett. **74**, 5112 (1995).
- [4] Tin-Lun Ho, Phys. Rev. Lett. **81**, 742 (1998); T. Ohmi and K. Machida, J. Phys. Soc. Jpn. **67**, 1822 (1998); S.-K. Yip, Phys. Rev. Lett. **83**, 4677 (1999); T. Isoshima, K. Machida, and T. Ohmi, J. Soc. Jpn. **70**, 1604 (2001); T. Mizushima, K. Machida and T. Kita, Phys. Rev. Lett. **89**, 030401 (2002); Tomoya Isoshima, and Kazushige Machida, Phys. Rev. A **66**, 023602 (2002); J.-P. Martikainen, A. Collin, and K.-A. Suominen, Phys. Rev. A **66**, 053604 (2002); T. Mizushima, K. Machida, and T. Kita, Phys. Rev. A **66**, 053610 (2002); T. Kita, T. Mizushima, and K. Machida, Phys. Rev. A **66**, 061601 (2002); J. W. Reijnders, F. J. M van Lankvelt, K. Schoutens, and N. Read, cond-mat/0306402.
- [5] E. J. Mueller, cond-mat/0309511; to appear in Physical Review A.
- [6] M. R. Matthews, B. P. Anderson, P. C. Haljan, D. S. Hall, C. E. Wieman, and E. A. Cornell, Phys. Rev. Lett. **83**, 2498 (1999)
- [7] A. E. Leanhardt, Y. Shin, D. Kielpinski, D. E. Pritchard, and W. Ketterle, Phys. Rev. Lett. **90**, 140403 (2003).
- [8] U. Al Khawaja and H. T. C. Stoof, Nature **411**, 918 (2001); U. Al Khawaja and H. T. C. Stoof Phys. Rev. A **64**, 043612 (2001); J. Ruostekoski and J. R. Anglin Phys. Rev. Lett. **86**, 3934 (2001); R. A. Battye, N. R. Cooper, and P. M. Sutcliffe, Phys. Rev. Lett. **88**, 080401 (2002); C. M. Savage and J. Ruostekoski Phys. Rev. Lett. **91**, 010403 (2003).
- [9] H. Schmaljohann, M. Erhard, J. Kronjäger, M. Kottke, S. van Staa, J. J. Arlt, K. Bongs, and K. Sengstock, cond-mat/0308281; M.-S. Chang, C. D. Hamley, M. D. Barrett, J. A. Sauer, K. M. Fortier, W. Zhang, L. You, M. S. Chapman. cond-mat/0309164.
- [10] Unlike the other experiments, reference [6] was able to perform *in-situ* imaging of the spin texture by taking advantage of the fact that the different pseudo-spin components actually belonged to different hyperfine levels.
- [11] W. Gerlach and O. Stern, Zeitschrift Für Physik, **9**, 349 (1922).
- [12] R. J. Epstein, I. Malajovich, R. K. Kawakami, Y. Chye, M. Hanson, P. M. Petroff, A. C. Gossard, and D. D. Awschalom, Phys. Rev. B **65**, 121202(R) (2002); R. K. Kawakami, Y. Kato, M. Hanson, I. Malajovich, J. M. Stephens, E. Johnston-Halperin, G. Salis, A. C. Gossard, D. D. Awschalom, Science **294**, 131 (2001).
- [13] S. Chandrasekhar, *Liquid Crystals*, Second Edition, Cambridge University Press, Cambridge (1992).
- [14] The Cartesian components  $\vec{\psi} = (\hat{\psi}_x, \hat{\psi}_y, \hat{\psi}_z)$  are related to the more familiar spherical components  $(\hat{\psi}_1, \hat{\psi}_0, \hat{\psi}_{-1})$  [where the subscript refers to the spin projection in the  $\hat{z}$  direction] by  $\hat{\psi}_x = (\hat{\psi}_1 - \hat{\psi}_{-1})/\sqrt{2}$ ,  $\hat{\psi}_y = i(\hat{\psi}_1 + \hat{\psi}_{-1})/\sqrt{2}$ ,  $\hat{\psi}_z = \hat{\psi}_0$ .
- [15] C. S. Adams and E. Riis, Prog. Quant. Electr. **21**, 1 (1997).
- [16] M. Born and E. Wolf, *Principles of optics*, Cambridge University Press, Cambridge (1959).
- [17] A. M. Dudarev, R. B. Diener, I. Carusotto, and Q. Niu, in preparation (2003).
- [18] V. B. Berestetskii, E. M. Lifshitz, and L. P. Pitaevskii, *Quantum Electrodynamics*, Pergamon Press, Oxford (1982), §49.
- [19] M. R. Andrews, M.-O. Mewes, N. J. van Druten, D. S. Durfee, D. M. Kurn, W. Ketterle, Science **273**, 84 (1996).
- [20] Absorption effects are included by changing the energy denominator in (3) to  $\omega - \omega_0 - i\Gamma/2$ . In the limit of large detuning,  $|\omega - \omega_0| \gg \Gamma$ , the  $c_i$  coefficients are real and the dielectric tensor is hermitian.
- [21] See, for instance, the Alkali D Line Data available at: <http://steck.us/alkalidata>.
- [22] After a tedious exercise in Clebsch-Gordon coefficients, one finds that for  $F = 1$  atoms with nuclear spin  $I = 3/2$   $c_1 = 2c_0$ , while  $c_1 = -c_0$  for atoms with  $I = 1/2$ .
- [23] This scaling relationship is derived in T. L. Ho and E. J. Mueller, Phys. Rev. Lett. **89**, 050401 (2002).
- [24] E. Demler and F. Zhou, Phys. Rev. Lett. **88** 163001, (2002).